Available online at BCREC website: https://bcrec.id

Bulletin of Chemical Reaction Engineering & Catalysis, 18 (3) 2023, 539-547

Research Article

Hydrazine-Fueled Solution Combustion Method: Fuel/Oxidizer Ratio Effects on Photocatalytic Performance of Bismuth Oxide

Yayuk Astuti[1*], Trie Nanda Mulyana[1], Brainy Happy Ana Tasiman[1], Adi Darmawan[1], Hendri Widiyandari[2]

[1]Chemistry Department, Faculty of Science and Mathematics, Universitas Diponegoro, Jl. Prof. Jacob Rais, Tembalang, Semarang 50275, Indonesia
[2]Physics Department, Faculty of Mathematics and Natural Sciences, Sebelas Maret University, Surakarta 57126, Indonesia

Received: 16th August 2023; Revised: 7th September 2023; Accepted: 8th September 2023
Available online: 10th October 2023; Published regularly: October 2023

Abstract

Bismuth oxide nanoparticles were synthesized through the solution combustion method with a variation of fuel: oxidizer (hydrazine: bismuth nitrate) ratios (ϕ) of ϕ<1, ϕ=1 (stoichiometrically balanced) and ϕ> 1. Bismuth oxide nanoparticles were characterized by Fourier Transform Infrared Spectroscopy (FTIR), X-Ray Diffraction (XRD), Scanning Electron Microscopy (SEM), and UV-Visible Diffuse Reflectance Spectroscopy (UV-DRS). The FTIR spectra obtained implies that the bismuth oxide nanoparticles of the three ratios contain Bi–O–Bi and Bi–O groups indicating its successful formation. XRD diffractogram suggests that the synthesized bismuth oxide nanoparticles form the α-Bi_2O_3 crystalline phase for ϕ<1 and ϕ>1; meanwhile a mixture of α-/β- Bi_2O_3 phases for ϕ=1. The SEM image illustrates that bismuth oxide nanoparticles form pebble shapes with the ratios in the order of increasing particle sizes of ϕ>1, ϕ=1, and ϕ<1. The UV-DRS results show that the bismuth oxide with ϕ<1, ϕ=1, and ϕ>1 have respective band gap energies of 2.76 eV, 2.72 eV, and 2.78 eV. The evaluation of the photocatalytic activity of the three bismuth oxide samples shows bismuth oxide with ϕ=1 has the highest photocatalytic activity in remazol black B and methyl orange dyes with rate constants 6.744 x 10-5 s^{-1} and 7.369 x 10-5 s^{-1}, respectively.

Keywords: Bismuth oxide; Solution Combustion; Fuel-oxidizer ratio; Photocatalyst

How to Cite: Y. Astuti, T. M. Mulyana, B. H. A. Tasiman, A. Darmawan, H. Widiyandari (2023). Hydrazine-Fueled Solution Combustion Method: Fuel/Oxidizer Ratio Effects on Photocatalytic Performance of Bismuth Oxide. *Bulletin of Chemical Reaction Engineering & Catalysis*, 18(3), 539-547 (doi: 10.9767/bcrec.19943)

Permalink/DOI: https://doi.org/10.9767/bcrec.19943

1. Introduction

Bismuth oxide is a semiconductor metal oxide that can be used as a photocatalyst because it has a band gap energy of 2.00-3.96 eV [1]. Bismuth oxide also has the advantage of having good optical and electrical properties, such as desirable refractive index, dielectric permittivity, photoluminescence, and good photoconductivity [2,3].

There are many methods available to synthesize bismuth oxide, such as solution combustion method [4–6], sol-gel method [7], biosynthesis involving tannic acid [8],

* Corresponding Author.
Email: yayuk.astuti@live.undip.ac.id (Y. Astuti);

microwave assisted method [9], hydrothermal method [10–14], chemical deposition [15], spray pyrolysis [16], electrospinning [17], and co-precipitation methods [18,19]. Among the methods available, solution combustion was chosen because it exhibits advantages such as low in cost, effortless, achieve better homogeneity than the final product, and able to produce very fine crystalline powder [20].

The solution combustion method comprises of two main components namely a fuel and oxidizer/oxidant. Oxidants are substances that contain certain metal cations and are used to provide metal elements into the final product. Bismuth nitrate is used because it is commercially available, water soluble and inexpensive [6]. Fuel is a substance that acts as a reducing agent. Hydrazine is often used as a fuel because it is a strong reducing agent, does not contain carbon elements, contains the amine group, and easy recharging [6,20]. Several studies have reported the use of hydrazine for synthesis of inorganic materials using solution combustion method such as CeO_2 [21], Fe_3O_4 and α-Fe_2O_3 [22], NiCu/CeO_2 [23]. Moreover, synthesis of bismuth oxide (Bi_2O_3) using hydrazine fueled-solution combustion has been conducted by Astuti *et al.* [24]. The product was then applied to degrade rhodamine B molecule dye under UV A light. The photocatalytic activity showed bismuth oxide degraded rhodamine B 40%. This result is far from the expectation. Therefore, another parameter influencing the characteristics and photocatalytic activity of the Bi_2O_3 synthesised using solution combustion method, that is, fuel/oxidizer should be explored. The fuel/oxidizer ratio is a parameter that can influence the surface area of the crystal, the crystal phase, pore and crystal size, which ultimately affects the ability of the bismuth oxide as a photocatalyst [25].

Research on the synthesis of bismuth oxide semiconductor with variations in the ratio of fuel-oxidizer has been widely carried out, but no research has been found to use hydrazine as a fuel and how it affects the ability of bismuth oxide as a photocatalyst. Thus, it encourages the research to synthesize bismuth oxide with variations in the ratio of fuel/oxidizer with hydrazine as the fuel and test the ability of the synthesized bismuth oxide photocatalyst. Furthermore, in this research, two different dyes solution remazol black B and methyl orange were used as pollutant models.

2. Materials and Methods

2.1 Materials

The materials used were $Bi(NO_3)_3.5H_2O \geq$ 98% (Sigma-Aldrich), HNO_3 65% (Merck), N_2H_4 (Merck) 80% in water, Remazol Black B dye ≥50% (Sigma-Aldrich), and Methyl Orange (Merck), distilled water.

2.2 Bismuth Oxide Synthesis

Synthesis was carried out with fuel-oxidizer ratios of (ϕ) = 0.8, 1 and 1.2. Bismuth nitrate pentahydrate was dissolved in 10 mL of 0.04 M nitric acid until homogeneous. The amount of bismuth nitrate pentahydrate dissolved depends on the fuel-oxidizer ratio (ϕ) to be made. Where for the fuel-oxidizer ratio (ϕ) = 0.8 the mass used was 1.45 g, (ϕ) = 1 was 1.81 g and (ϕ) = 1.2 was 2.18 g.

Subsequently, 0.0313 mL of hydrazine was added as fuel. The mixture was then stirred for 5 minutes and was later heated for 8 hours at 300 °C on a hotplate stirrer (Thermoscientific Cimarec SP88857105). The formed product was calcined for 4 hours using a furnace (Thermoscientific Thermolyne Benchtop Muffle Furnace FB1310M-22) at 700 °C.

2.3 Characterizations

Bismuth oxide nanoparticles were extensively characterized. The crystal functional groups were identified by using Fourier Transform Infrared Spectroscopy (Shimadzu IRAffinity-1 FT-IR), the crystal phase and compositions were analyzed using X-Ray diffraction (XRD Shimadzu 7000), the three-dimensional crystal structure was analyzed using Scanning Electron Microscopy (SEM JEOL JED 6510LA), and the value of the band gap was analyzed using UV-Vis Diffuse Reflectance Spectroscopy (Pharmaspec UV-DRS UV 1700).

2.4 Photocatalytic Activity Test

The photocatalytic ability of the bismuth oxide was explored by its application in degrading dyes (rhemazol black B and methyl orange). The working solutions used were 50 mL of 25 ppm RBB and 50 mL of 5 ppm MO. Each of the working solution was put into the photocatalyst reactor and then stirred using over a variation of time durations. The sample was analyzed using a UV-Vis spectrophotometer. The final step is calculation of degradation percentage after photocatalytic process using this formula:

$$Degradation\ Percentage\ (\%) = \frac{C_0 - C_t}{C_0} x100\% \quad (1)$$

with C_o = initial concentration of dye (ppm), C_t = final concentration of dye (ppm) at t time.

3. Results and Discussion

3.1 Bismuth Oxide Synthesis

The synthesis using varying ratios of fuel-oxidant obtained bismuth oxide products that are yellow in color. According to Deshpande *et al*. [26], the reactions that took place during the synthesis are as follows:

(a) Fuel/Oxidant ratio of 0.8:

$$2Bi(NO_3)_3.5H_2O + 6N_2H_4 + (-1.5)O_2 \rightarrow Bi_2O_3 + 22H_2O + 9N_2 \quad (2)$$

(b) Fuel/Oxidant ratio of 1.0:

$$4Bi(NO_3)_3.5H_2O + 15N_2H_4 \rightarrow 2Bi_2O_3 + 50H_2O + 21N_2 \quad (3)$$

(c) Fuel/Oxidant ratio of 1.2:

$$2Bi(NO_3)_3.5H_2O + 9N_2H_4 + (1.5)O_2 \rightarrow Bi_2O_3 + 28H_2O + 12\ N_2 \quad (4)$$

Heating at a temperature of 300 °C for 8 hours was done to initiate the solution combustion reaction so that the fuel and the oxidant would be closely associated in the gel network [6]. The heating produced a white powder, N_2 gas and H_2O gas. The resulting white powder (Figure 1) was bismuth oxide that had not been completely formed because there were still parts that had not undergone completely burning [25] in addition to it not containing C atoms that would generally produce black color when burned.

Calcination for 4 hours at 700 ˚C was done to ensure that all the synthesis materials reacted. The powder obtained from the heating was calcined for 4 hours at a temperature of 700 °C. It acquired pale yellow color (Figure 2) as what is generally a property of a bismuth oxide.

3.2 Characterizations

3.2.1 FTIR characterization

FTIR characterization allows the identification the groups contained in the synthesized bismuth oxide. The bismuth oxide spectra before calcination (Figure 3) shows the presence of pure bismuth oxide formed along with indications of impurities still contained.

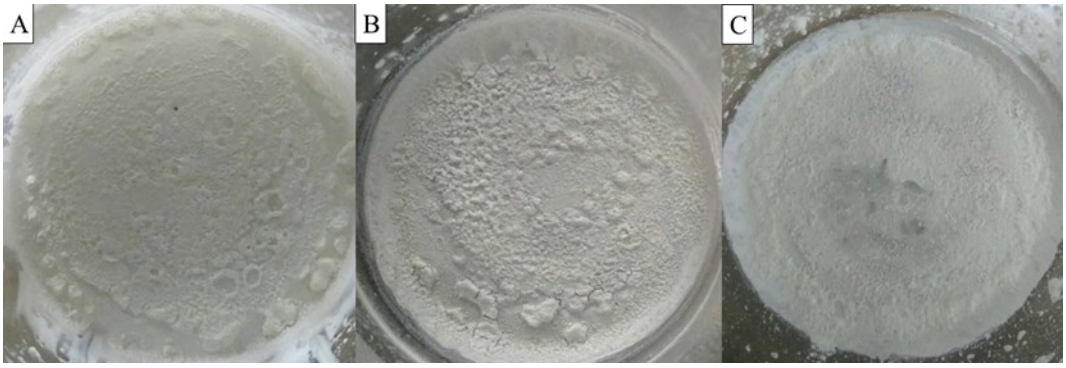

Figure 1. Products synthesized with different ratio of fuel/oxidant (a) ϕ=0.8; (b) ϕ=1 and (c) ϕ=1.2 after 8 hours heating

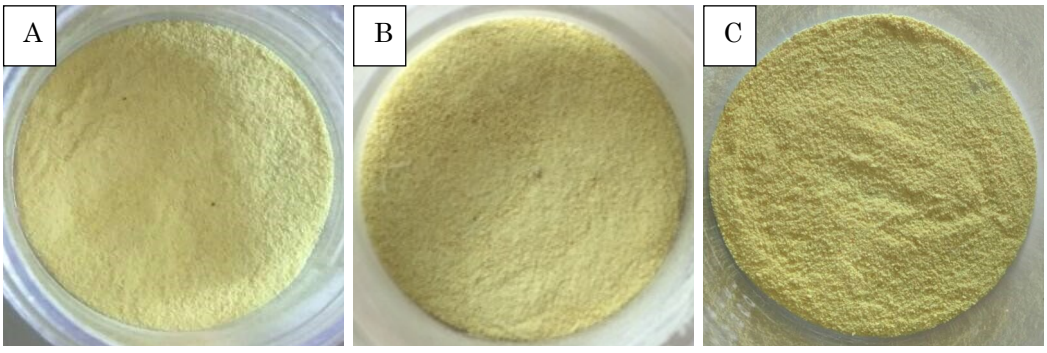

Figure 2. Products after calcination using fuel/ratio (a) ϕ=0.8; (b) ϕ=1; and (c) ϕ=1.2

Bismuth oxides formed were denoted by the peaks at 813.12, 811.00, and 812.42 cm^{-1} signifying the Bi–O–Bi bond [27] as well as the peaks at 1303.59, 1321.00, and 1280.6 cm^{-1} signifying the stretching of Bi–O [27] for the ratios of 0.8, 1.0, and 1.2, respectively. The impurities identified consisted of the $–NO_3$ group (1300-1400 cm^{-1}) [28], suggesting that the bismuth oxide had not undergone complete formation, the –NH group at 1032.40, 1034.00, and 1031.04 cm^{-1} similar to that in hydrazine (1063.80 cm^{-1}), and the NH_2 group with scissoring vibrations at 1586.67 and 1621.00 cm^{-1} also similar to that in hydrazine (1612.73 cm^{-1}) [29] inferring that hydrazine had not reacted completely, and the –OH group bending around the 3786, 3751, and 3789.83 cm^{-1} wavenumbers [30] denoting the presence of solvents indicating that further calcination was necessary.

The bismuth oxide spectra after calcination (Figure 4) shows the formation of bismuth oxide at peaks of 829.53 (ratio 0.8), 838 (ratio 1), 829.03 (ratio 1.2) and 839 cm^{-1} (pure) denoting the Bi–O–Bi bonding [27] and peaks at 1328.63 (ratio 0.8), 1383.68 (ratio 1), 1328.70 (ratio 1.2) and 1384 cm^{-1} (pure) for the stretching of Bi–O [27]. Impurities, such as $–NO_3$, –NH, and –OH, experienced reduction in respect to the conditions prior to calcination.

3.2.2 XRD characterization

XRD characterization is able to determine the crystalline phase of the synthesized bismuth oxide. Similarities of the synthesized products synthesized with the standard Bi_2O_3 were identified using the Match software. The 2θ values obtained from the characterization were compared with the Joint Committee on Powder Diffraction Standards (JCPDS) database (α-Bi_2O_3 (JCPDF No. 41-1449), ß-Bi_2O_3 (JCPDF No. 76-0147), and γ-Bi_2O_3 (JCPDF No. 45-1344)).

XRD diffractogram of the synthesized bismuth oxide synthesized (Figure 5) shows that ratios 0.8 and 1.2 are of α-Bi_2O_3 (monoclinic) whereas ratio 1 is a mixture of α-Bi_2O_3 (monoclinic) and *β*-Bi_2O_3 (tetragonal). The Match software detailed that the similarity of α-Bi_2O_3 [31] with the synthesized bismuth oxides of the ratio 1.2 amounts to 99.21%, 96.81% for the ratio 1, 94.94% for the ratio 0.8. Thus, it can be concluded that bismuth oxides synthesized have high purity and crystallinity. Moreover, the crystallite size of the particles of every product calculated using Scherer equation can be seen in Table 1. Lattice parameters calculated using Match software show a value of a = 5.85 Å; b = 8.17 Å; c = 7.51 Å with an angle of 113°.

Table 1. Crystallite size of the products

Bismuth oxide synthesized using different ratio fuel/oxidizer (ϕ)	Crystallite size
ϕ = 0.8	65.26 nm
ϕ = 1.0	69.60 nm
ϕ = 1.2	75.48 nm

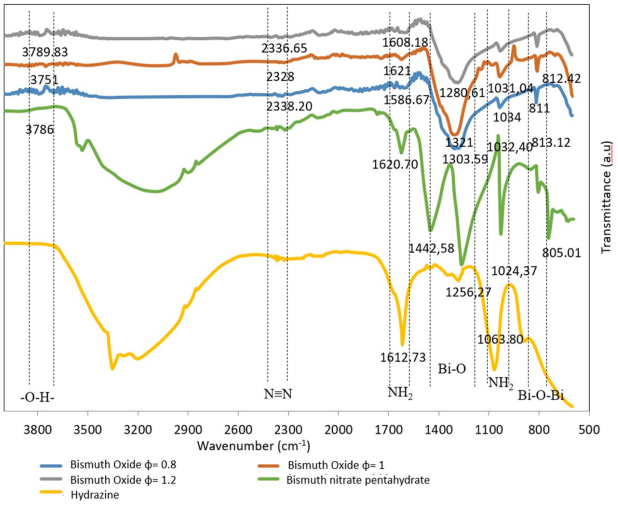

Figure 3. FTIR spectra of precursors and products before calcination with ratio of fuel/oxidant ϕ=0.8; ϕ=1; and ϕ=1.2

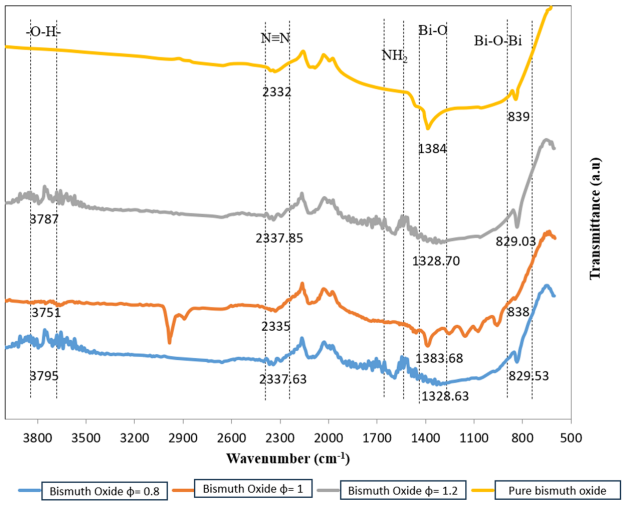

Figure 4. FTIR spectra of pure bismuth oxide and products after calcination with ratio of fuel/oxidant ϕ=0.8; ϕ=1; and ϕ=1.2

3.2.3 SEM characterization

SEM characterization was done to determine the three-dimensional structure of the synthesized bismuth oxides. The SEM image at 1000x magnification (Figure 6 a. Ratio 0.8 b. Ratio 1.2 and c. Ratio 1) shows that the morphologies of the three bismuth oxide samples are comparable to gravel. The bismuth oxide with the ratio of 1.2 has the smallest size of 18.902 – 38.369 µm followed by the ratio of 1 (9.143 – 30.695 µm), and the ratio of 0.8 (25.31 – 110.983 µm).

According to the findings presented in Figure 6 from the SEM analysis, when comparing a ratio of 1.2 to a ratio of 1, it is observed that the particle size of bismuth oxide is slightly smaller in the former case, although the distinction is not particularly pronounced. It is worth noting that a catalyst's photocatalytic activity tends to increase with a larger surface area.

3.2.4 UV-DRS characterization

Band gap values were determine based on the Tauc Plot calculation by graphing the relationship between hv as the x-axis and $(ahv)^2$ as the y-axis then extrapolating the straight line on the hv vs $(ahv)^2$ graph until it intersects the hv or E_g axis (x-axis) [32]. The band gaps are shown in the graph in Figure 7

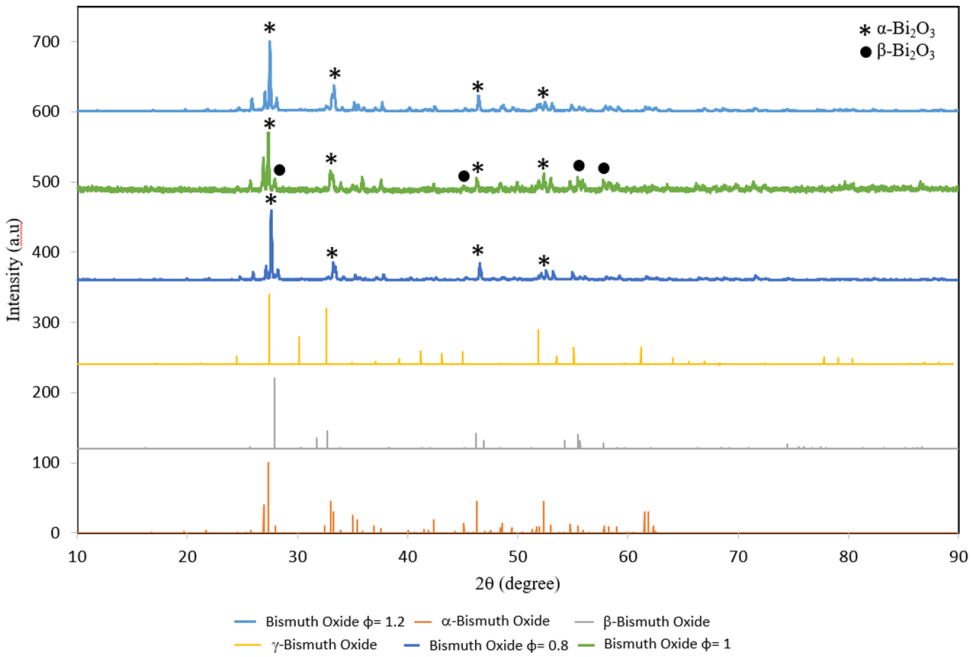

Figure 5. XRD diffractograms of resulting products

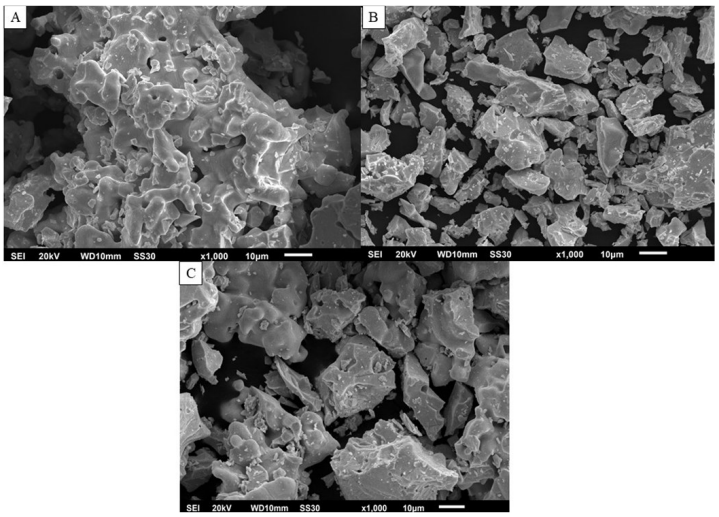

Figure 6. SEM images of bismuth oxide synthesized using fuel/oxidant ratio (a) ϕ=0.8; (b) ϕ=1; and (c) ϕ=1.2 with 1000x magnification

(a. Ratio 0.8 b. Ratio 1 c. Ratio 1.2), with values for ratio of 0.8 of 2.76 eV, ratio of 1 of 2.72 eV, and ratio of 1.2 of 2.78 eV.

3.3 Photocatalytic Activity

Testing of this particular activity was done to determine the ability of the synthesized bismuth oxide as a photocatalyst. The observations on the effect of the duration of photocatalysis on the remazol black B (RBB) (Figure 8a) and the methyl orange (MO) (Figure 8b) concentrations demonstrate that the concentration of the degraded dyes increases with photocatalysis time. This is due to the longer irradiation time, allowing more photons to be in contact with the system.

The degradation activities on remazol black B (Figure 9a) and methyl orange (Figure 9b) dyes by bismuth oxide have been calculated by a first order kinetics reaction. The slope values of the graphs signify the constant rates of the degradation reactions of the dyes. The values of the RBB degradation rate constants of bismuth oxides of ratio 0.8, ratio 1 and ratio 1.2 are 2.058×10^{-5} s^{-1}, 6.744×10^{-5} s^{-1}, 3.708×10^{-5} s^{-1}. The values of the MO degradation rate constants of bismuth oxides with ratio of 0.8, 1, and 1.2 are 1.805×10^{-5} s^{-1}, 7.369×10^{-5} s^{-1}, 5.733×10^{-5} s^{-1}. Based on these reaction rate constants, it can be established that the bismuth oxide ratio 1 has the highest photocatalytic activity.

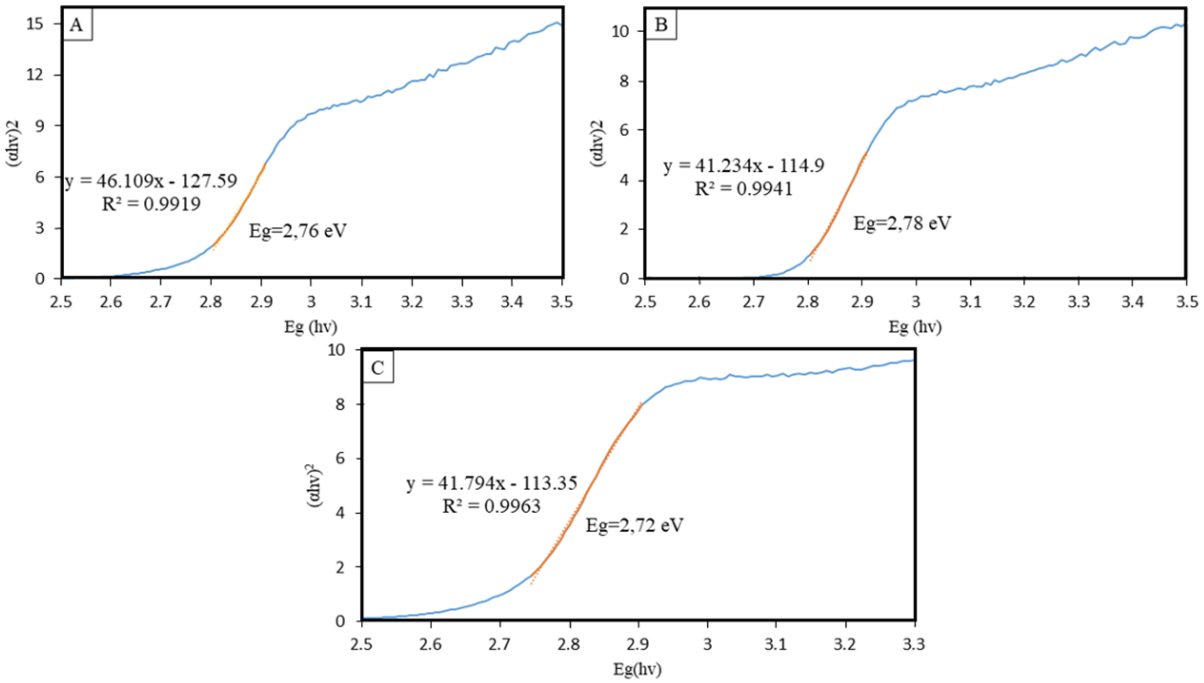

Figure 7. DRS UV spectra of bismuth oxide synthesized using fuel/oxidant ratio (a) ϕ=0.8; (b) ϕ=1; and (c) ϕ=1.2

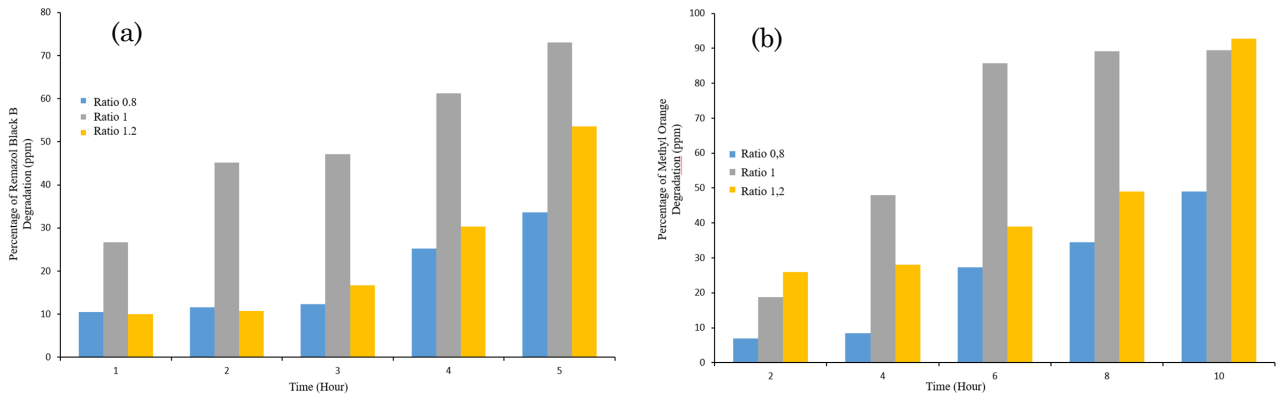

Figure 8. Photocatalytic time effect on the percentage of (a) RBB and (b) MO degraded by bismuth oxide synthesized with different fuel/oxidant ratio

The mechanism of degradation of dyes by bismuth oxide can be understood in the following reaction sequence:

$Bi_2O_3 + h\upsilon \rightarrow Bi_2O_3 + e^-_{cb} + h^+_{vb}$
$H_2O + h^+ \rightarrow \cdot OH + H^+$
$O_2 + e^- \rightarrow \cdot O_2^-$
$\cdot O_2^- + H^+ \rightarrow HO_2\cdot$
$2HO_2\cdot \rightarrow O_2 + H_2O_2$
$H_2O_2 + \cdot O_2^- \rightarrow \cdot OH + OH^- + O_2$
dyes + $\cdot OH$ + $\cdot O_2^- \rightarrow CO_2 + H_2O$

when, the Bi_2O_3 was illuminated by light, the electron will be excited from valance band to conduction band and leave positive hole in valance band. Positive hole will produce ·OH and H^+. Meanwhile, the electrons in the conduction band would react with atmospheric O_2 to form $\cdot O_2$. $\cdot O_2$ could also serve as a source in the formation of ·OH through a protonation process. The ·OH could oxidize the dye molecule into simpler compounds, namely CO_2 and H_2O [14].

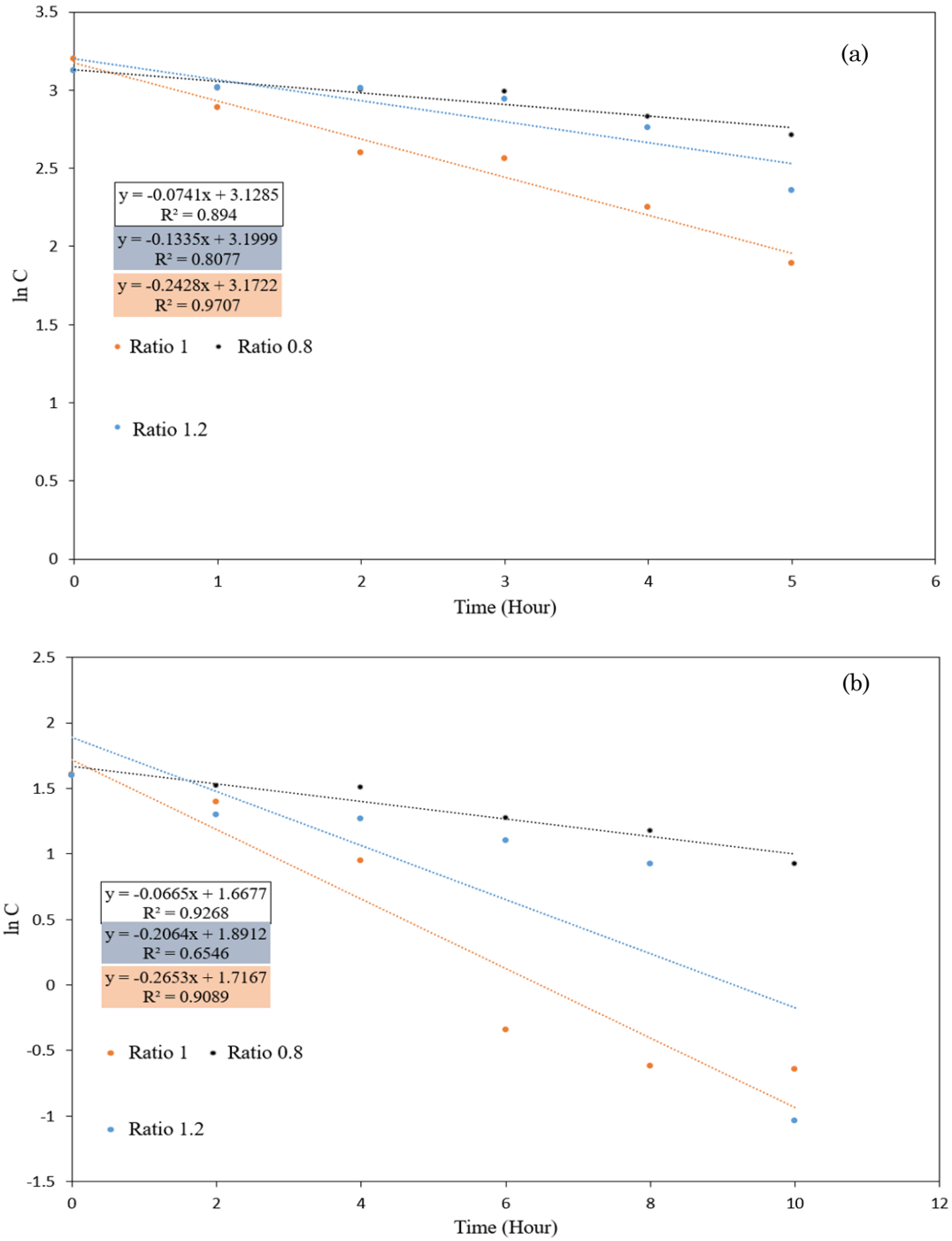

Figure 9. First order kinetics of (a) RBB and (b) MO photocatalytic degradation

4. Conclusion

Bismuth oxide has been successfully synthesized using the solution combustion method. FTIR characterization results show that bismuth oxides were formed as proven by the peaks at 829.53 (ratio 0.8); 838 (ratio 1); 829.03 (ratio 1.2) denoting the Bi–O–Bi bond and peaks at 1328.63 (ratio 0.8); 1383.68 (ratio 1); 1328.70 (ratio 1.2) denoting Bi–O stretching. XRD results suggest that bismuth oxide with ratios of 0.8 and 1.2 exhibit α-Bi_2O_3 phase while the ratio of 1 contains a mixture of α-Bi_2O_3 and ß-Bi_2O_3 phases. SEM images show that the bismuth oxides synthesized have shapes similar to gravel with the ratio 1.2 having the smallest size followed by ratio 1 and ratio 0.8. The UV-DRS results show that the Bi_2O_3 with ratios of 0.8, 1 and 1.2 have respective energy band gaps of 2.76 eV, 2.72 eV and 2.78 eV. Bismuth oxides synthesized can be used as a photocatalyst with the ratio 1 having the highest photocatalytic activity in degrading RBB and MO.

Acknowledgement

The authors would like to thank Universitas Diponegoro, for financial support through *Riset Kolaborasi Indonesia* (RKI) grant in the fiscal year 2022 with the grant no. 432-06/UN7.D2/PP/VI/2022.

CRediT Author Statement

Author Contributions: *Astuti, Y.*: Conceptualization, Methodology, Investigation, Resources, Data Curation, Writing, Review and Editing, Supervision; *Mulyana, T. R.*: Experiment, Formal Analysis, Data Curation, Writting Draft Preparation; *Tasiman, B. H. A.*: Validation, Review and Editing, Data Curation; Darmawan, A: Review and Editing, Validation; *Widiyandari, H.*: Investigation, Resources, Writing, Review and Editing Validation. All authors have read and agreed to the published version of the manuscript.

References

[1] Jiang, S., Wang, L., Hao, W., Li, W., Xin, H., Wang, W., Wang, T. (2015). Visible-Light Photocatalytic Activity of S-Doped α-Bi_2O_3. *Journal of Physical Chemistry C*, 119(25), 14094–14101. DOI: 10.1021/jp5117036

[2] M. Mallahi, A. Shokuhfar, M. R. Vaezi, A. Esmaeilirad, V. Mazinani. (2014). Synthesis and characterization of Bismuth oxide nanoparticles via sol-gel. *American Journal of Engineering Research (AJER)*, 03, 162–165. www.ajer.org

[3] Schmidt, S., Kubaski, E.T., Volanti, D.P., Sequinel, T., Bezzon, V.D.N., Beltrán, A., Tebcherani, S.M., Varela, J.A. (2015). Effect of Pressure-Assisted Heat Treatment on Photoluminescence Emission of α-Bi_2O_3 Needles. *Inorganic Chemistry*, 54(21), 10184–10191. DOI: 10.1021/acs.inorgchem.5b01237

[4] Astuti, Y., Fauziyah, A., Nurhayati, S., Wulansari, A.D., Andianingrum, R., Hakim, A.R., Bhaduri, G. (2016). Synthesis of α-Bismuth oxide using solution combustion method and its photocatalytic properties. *IOP Conference Series: Materials Science and Engineering*, 107(1). DOI: 10.1088/1757-899X/107/1/012006

[5] Carlos, E., Martins, R., Fortunato, E., Branquinho, R. (2020). Solution combustion synthesis: towards a sustainable approach for metal oxides. *Chemistry–A European Journal*, 26(42), 9099–9125. DOI: 10.1002/chem.202000678.

[6] Deganello, F., Tyagi, A.K. (2018). Solution combustion synthesis, energy and environment: Best parameters for better materials. In *Progress in Crystal Growth and Characterization of Materials*, 64(2), 23–61. DOI: 10.1016/j.pcrysgrow.2018.03.00

[7] Astuti, Y., Listyani, B.M., Suyati, L., Darmawan, A. (2021). Bismuth oxide prepared by sol-gel method: variation of physicochemical characteristics and photocatalytic activity due to difference in calcination temperature. *Indonesian Journal of Chemistry*, 21(1), 108–117. DOI: 10.22146/ijc.53144.

[8] Ascencio Aguirre, F.M., Herrera Becerra, R. (2015). New synthesis of bismuth oxide nanoparticles Bi_2O_3 assisted by tannic acid. *Applied Physics A: Materials Science and Processing*, 119(3), 909–915. DOI: 10.1007/s00339-015-9039-x

[9] Marks, M., Jeppesen, H.S., Lock, N. (2022) Tuneable phase, morphology, and performance of bismuth oxyhalide photocatalysts via microwave-assisted synthesis. *ACS Appl. Mater. Interfaces*, 14(20), 23496–23506. DOI: 10.1021/acsami.2c03837.

[10] Astuti, Y., Latifah, A., Arnelli., Suseno, A., Lestariningsih, T. (2023) Bismuth sulfide/coconut fiber based-activated carbon composite: synthesis, characterization, and electrochemical performance. *Emergent Mater.*, 1–13. DOI: 10.1007/s42247-023-00529-5.

[11] Astuti, Y., Mei, R., Darmawan, A., Arnelli, A., Widiyandari, H. (2022) Enhancement of electrical conductivity of bismuth oxide/activated carbon composite. *Scientia Iranica*, 29(6), 3119–3131. DOI: 10.24200/SCI.2022.57674.5359.

[12] Astuti, Y., Farihah, D.N., Ekaningsih, A.Z., Darmawan, A. (2023). Electrochemical performance of one-pot hydrothermal-derived bismuth oxide/commercial activated carbon/graphite composite. *Materials Science and Technology*, 1–14. DOI: 10.1080/02670836.2023.2184574.

[13] Astuti, Y., Hartinah, S., Darmawan, A., Widiyandari H. (2022). Synthesis and characterization of bismuth oxide/commercial activated carbon composite for battery anode. *Open Chem*, 20(1), 1476–1484. DOI: 10.1515/chem-2022-0247.

[14] Astuti, Y., Musthafa, F., Arnelli, A., Nurhasanah, I. (2022). French Fries-Like Bismuth Oxide: Physicochemical Properties, Electrical Conductivity and Photocatalytic Activity. *Bulletin of Chemical Reaction Engineering & Catalysis*, 17(1), 146–156. DOI: 10.9767/BCREC.17.1.12554.146-156

[15] Gujar, T.P., Shinde, V.R., Lokhande, C.D., Mane, R.S., Han, S.-H. (2005). Bismuth oxide thin films prepared by chemical bath deposition (CBD) method: annealing effect, *Appl. Surf. Sci.*, 250(1–4), 161–167. DOI: 10.1016/j.apsusc.2004.12.050.

[16] Ambare, R.C., Shinde, P., Nakate, U.T., Lokhande, B.J., Mane, R.S. (2018). Sprayed bismuth oxide interconnected nanoplate supercapacitor electrode materials. *Appl. Surf. Sci.*, 453, 214–219. DOI: 10.1016/j.apsusc.2018.05.090.

[17] Demir, E., Soytas, S.H., Demir-Cakan, R. (2019). Bismuth oxide nanoparticles embedded carbon nanofibers as self-standing anode material for Na-ion batteries. *Solid State Ion*, 342, 115066. DOI: 10.1016/j.ssi.2019.115066.

[18] Puttaraju, T.D., Shashank, M., Naika, H.R., Nagaraju, G., Manjunatha, M. (2022). Synthesis of bismuth oxychloride nanoparticles via co-precipitation method: Evaluation of photocatalytic activity. *Mater. Today Proc.*, 62, 5533–5539. DOI: 10.1016/j.matpr.2022.04.333.

[19] Kiran, V.S., Sumathi, S. (2017). Comparison of catalytic activity of bismuth substituted cobalt ferrite nanoparticles synthesized by combustion and co-precipitation method. *Journal of Magnetism and Magnetic Materials*, 421, 113–119. DOI: 10.1016/j.jmmm.2016.07.068.

[20] Alves, A.K., Bergmann, C.P., Berutti, F.A. (2013). Novel synthesis and characterization of nanostructured materials. Springerlink, DOI: 10.1007/978-3-642-41275-2.

[21] Kang, W., Ozgur, D.O., Varma, A. (2018). Solution combustion synthesis of high surface area CeO_2 nanopowders for catalytic applications: reaction mechanism and properties. *ACS Appl. Nano Mater.*, 1(2), 675–685. DOI: 10.1021/acsanm.7b00154

[22] Toniolo, J., Takimi, A.S., Andrade, M.J., Bonadiman, R., Bergmann, C.P. (2007). Synthesis by the solution combustion process and magnetic properties of iron oxide (Fe_3O_4 and α-Fe_2O_3) particles. *Journal of Materials Science*, 42(13), 4785–4791. DOI: 10.1007/s10853-006-0763-7

[23] Kang, W., Guo, H., Varma, A. (2019). Noble-metal-free $NiCu/CeO_2$ catalysts for H_2 generation from hydrous hydrazine. *Appl. Catal. B*, 249, 54–62 DOI: 10.1016/j.apcatb.2019.02.066

[24] Astuti, Y., Elesta, P.P., Widodo, D.S., Widiyandari, H., Balgis, R. (2020). Hydrazine and urea fueled-solution combustion method for Bi_2O_3 synthesis: Characterization of physicochemical properties and photocatalytic activity. *Bulletin of Chemical Reaction Engineering & Catalysis*, 15(1), 104–111. DOI: 10.9767/bcrec.15.1.5483.104-111

[25] Jadhav, L.D., Patil, S.P., Jamale, A.P., Chavan, A.U. (2013) Solution combustion synthesis: Role of oxidant to fuel ratio on powder properties. *Materials Science Forum*, 85–98. DOI: 10.4028/www.scientific.net/MSF.757.85.

[26] Deshpande, K., Mukasyan, A., Varma, A. (2004). Direct synthesis of iron oxide nanopowders by the combustion approach: reaction mechanism and properties. *Chemistry of materials*, 16(24), 4896–4904. DOI: 10.1021/cm040061m.

[27] Bandyopadhyay, S., Dutta, A. (2017). Thermal, optical and dielectric properties of phase stabilized δ – Dy-Bi_2O_3 ionic conductors. *Journal of Physics and Chemistry of Solids*, 102, 12–20. DOI: 10.1016/j.jpcs.2016.11.001.

[28] Nandiyanto, A.B.D., Oktiani, R., Ragadhita, R. (2019). How to read and interpret FTIR spectroscope of organic material. *Indonesian Journal of Science and Technology*, 4(1), 97–118. DOI: 10.17509/ijost.v4i1.15806

[29] Chuang, C.C., Shiu, J.S., Lin, J.L. (2000). Interaction of hydrazine and ammonia with TiO_2. *Physical Chemistry Chemical Physics*, 2(11), 2629–2633. DOI: 10.1039/B001389G.

[30] Greever, J.C. (1995). Organic Chemistry. ACS Publications, 1995.

[31] Malmros, G. (1970). The crystal structure of a-Bi_2O_3. *Acta Chem. Scand.*, 24(2), 384.

[32] Ebraheem, S., El-Saied, A. (2013). Band gap determination from diffuse reflectance measurements of irradiated lead borate glass system doped with TiO_2 by using diffuse reflectance technique. DOI: 10.4236/msa.2013.45042.